Coupled-Strip-Transmission-Line Filters and Directional Couplers

E. M. T. JONES† AND J. T. BOLLJAHN†

Summary—**This paper describes the theory of operation of coupled strip line filters and directional couplers, and presents information from which these components may be easily designed. Low-pass, band-pass, all-pass, and all-stop filter characteristics are obtained from these coupled lines either by placing open or short circuits at two of the four available terminal pairs, or by interconnecting two of the terminal pairs. Directional couplers having perfect directivity and constant input impedance at all frequencies, and for all degrees of coupling, are obtained by placing equal resistive loads at each of the four terminal pairs.**

Introduction

THE ELECTROMAGNETIC COUPLING that exists between parallel transmission lines has been used to advantage by a number of investigators to construct filters and directional couplers from coupled open-wire transmission lines, and coupled coaxial lines.[1–5] This natural coupling can be used equally well in the construction of shielded strip transmission line filters and directional couplers. This paper derives formulas from which these coupled-strip-line filters and coupled-strip-line directional couplers may be designed.

Coupled Transmission-Line Impedance and Admittance Matrices

The general physical configuration of coupled strip lines to be considered here is illustrated in Fig. 1. A convenient way to describe the behavior of these coupled strip transmission lines is by means of the impedance matrix which will now be derived. Consider the shielded coupled transmission lines shown in Fig. 1, where the two transmission lines are supported midway between the two ground planes and are driven by a set of five constant-current generators at each end. The four current generators $i_1/2$ energize the even or unbalanced mode on the structure producing voltages on the two conductors of the form

$$v_{a_1}(z) = v_{b_1}(z) = -jZ_{oe}i_1 \frac{\cos k(l-z)}{\sin kl}, \tag{1}$$

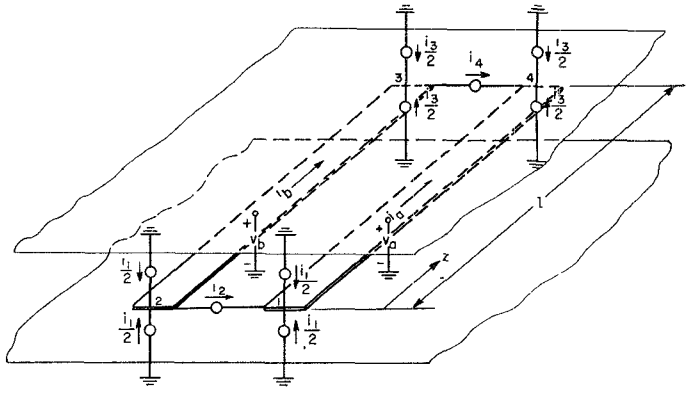

Fig. 1.—Notation used in deriving the impedance matrix of coupled transmission lines.

where

Z_{oe} = characteristic impedance of one wire to ground with equal currents in the same direction.

Likewise, the current generators $i_3/2$ produce voltages on the two conductors

$$v_{a_3}(z) = v_{b_3}(z) = -jZ_{oe}i_3 \frac{\cos kz}{\sin kl}. \tag{2}$$

The current generators i_2 and i_4 produce odd or balanced voltages on the lines of the form

$$v_{a_2}(z) = -v_{b_2}(z) = -jZ_{oo}i_2 \frac{\cos k(l-z)}{\sin kl}, \tag{3}$$

and

$$v_{a_4}(z) = -v_{b_4}(z) = -jZ_{oo}i_4 \frac{\cos kz}{\sin kl}, \tag{4}$$

where

Z_{oo} = characteristic impedance of one wire to ground with equal currents in opposite directions.

The total current and voltage at each of the terminals (1, 2, 3, and 4) are easily related to the currents and voltages of the even- and odd-mode excitation. Assume that the positive current in each case is into a terminal; then the terminal currents are

$$\begin{aligned} I_1 &= i_1 + i_2 \\ I_2 &= i_1 - i_2 \\ I_3 &= i_3 - i_4 \\ I_4 &= i_3 + i_4. \end{aligned} \tag{5}$$

† Stanford Research Institute Menlo Park, Calif.

[1] A. Alford, "Coupled networks in radio-frequency circuits," PROC. IRE, vol. 29, pp. 55–70; February, 1941.
[2] J. J. Karakash and D. E. Mode, "A coupled coaxial transmission-line band-pass filter," PROC. IRE, vol 38, pp. 48–52; January, 1950.
[3] W. L. Firestone, "Analysis of transmission line directional couplers," PROC. IRE, vol. 42, pp. 1529–1538; October, 1954.
[4] B. M. Oliver, "Directional electromagnetic couplers," PROC. IRE, vol. 42, pp. 1686–1692; November, 1954.
[5] R. C. Knechtli, "Furtheranalysis of transmission-line directional couplers," PROC. IRE, vol. 43, pp. 867–869; July, 1955.

FILTER	Z_I	α, β and θ_c
1- LOW PASS 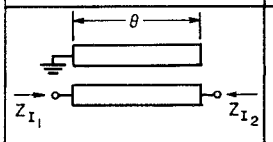	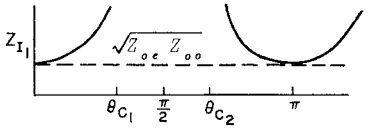 $Z_{I_1} = \dfrac{2 Z_{oe} Z_{oo} \cos\theta}{[-(Z_{oe} - Z_{oo})^2 + (Z_{oe} + Z_{oo})^2 \cos^2\theta]^{1/2}}$ $Z_{I_2} = \dfrac{Z_{oe} Z_{oo}}{Z_{I_1}}$	$\cosh(\alpha + j\beta) = \dfrac{[(Z_{oe} + Z_{oo})^2 \cos^2\theta - (Z_{oe} - Z_{oo})^2]^{1/2}}{2\sqrt{Z_{oe} Z_{oo}}}$ $\cos\theta_{c_1} = -\cos\theta_{c_2} = \left[\dfrac{\frac{Z_{oe}}{Z_{oo}} - 1}{\frac{Z_{oe}}{Z_{oo}} + 1}\right]$
2-BAND PASS 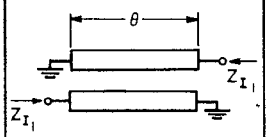	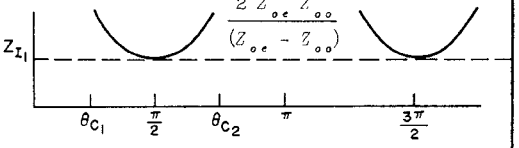 $Z_{I_1} \dfrac{2 Z_{oe} Z_{oo} \sin\theta}{[(Z_{oe} - Z_{oo})^2 - (Z_{oe} + Z_{oo})^2 \cos^2\theta]^{1/2}}$	$\cosh(\alpha + j\beta) = \left[\dfrac{\frac{Z_{oe}}{Z_{oo}} + 1}{\frac{Z_{oe}}{Z_{oo}} - 1}\right] \cos\theta$ $\cos\theta_{c_1} = -\cos\theta_{c_2} = \left[\dfrac{\frac{Z_{oe}}{Z_{oo}} - 1}{\frac{Z_{oe}}{Z_{oo}} + 1}\right]$
3-BAND PASS 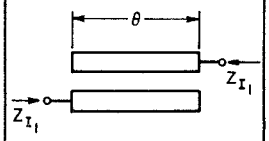	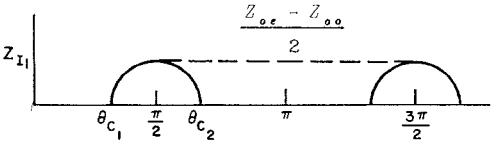 $Z_{I_1} = \dfrac{[(Z_{oe} - Z_{oo})^2 - (Z_{oe} + Z_{oo})^2 \cos^2\theta]^{1/2}}{2 \sin\theta}$	$\cos\theta_{c_1} = -\cos\theta_{c_2} = \left[\dfrac{\frac{Z_{oe}}{Z_{oo}} - 1}{\frac{Z_{oe}}{Z_{oo}} + 1}\right]$ $\cosh(\alpha + j\beta) = \left[\dfrac{\frac{Z_{oe}}{Z_{oo}} + 1}{\frac{Z_{oe}}{Z_{oo}} - 1}\right] \cos\theta$

Fig. 2(a)

CASE	Z_I	α, β and θ_c
4-BAND PASS 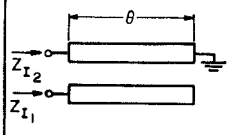	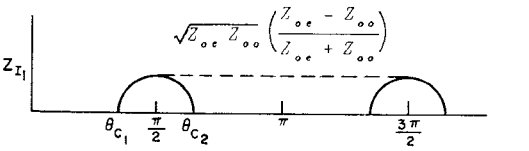 $Z_{I_1} = \dfrac{\sqrt{Z_{oe} Z_{oo}}\,[(Z_{oe} - Z_{oo})^2 - (Z_{oe} + Z_{oo})^2 \cos^2\theta]^{1/2}}{\sin\theta\,(Z_{oe} + Z_{oo})}$ $Z_{I_2} = \dfrac{Z_{oe} Z_{oo}}{Z_{I_1}}$	$\cosh(\alpha + j\beta) = \dfrac{1}{\sin\theta}\left[1 - \left(\dfrac{Z_{oe} + Z_{oo}}{Z_{oe} - Z_{oo}}\right)^2 \cos^2\theta\right]^{1/2}$ $\cos\theta_{c_1} = -\cos\theta_{c_2} = \left[\dfrac{\frac{Z_{oe}}{Z_{oo}} - 1}{\frac{Z_{oe}}{Z_{oo}} + 1}\right]$
5- ALL PASS 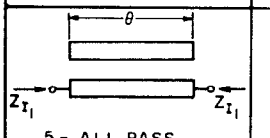	$Z_{I_1} = \dfrac{Z_{oe} + Z_{oo}}{2}$	$\beta = \theta$
6- ALL PASS 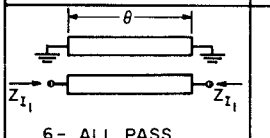	$Z_{I_1} = \dfrac{2 Z_{oe} Z_{oo}}{Z_{oe} + Z_{oo}}$	$\beta = \theta$
7- ALL PASS 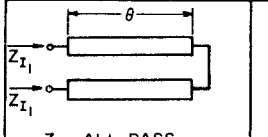	$Z_{I_1} = \sqrt{Z_{oe} Z_{oo}}$	$\cos\beta = \dfrac{\frac{Z_{oe}}{Z_{oo}} - \tan^2\theta}{\frac{Z_{oe}}{Z_{oo}} + \tan^2\theta}$

Fig. 2(b)

CASE	Z_I	α, β, v_c
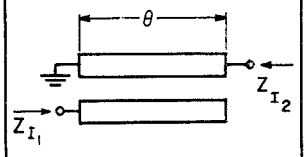 8-ALL STOP	$Z_{I_1} = -j\dfrac{2Z_{oo}Z_{oe}}{Z_{oo}+Z_{oe}}\cot\theta$ $Z_{I_2} = \dfrac{Z_{oe}Z_{oo}}{Z_{I_1}}$	$\alpha = \infty$
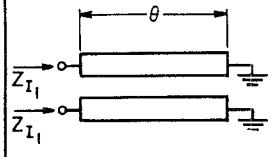 9-ALL STOP	$Z_{I_1} = j\sqrt{Z_{oe}Z_{oo}}\tan\theta$	$\cosh\alpha = \dfrac{Z_{oe}+Z_{oo}}{Z_{oe}-Z_{oo}}$
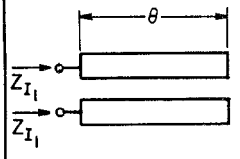 10-ALL STOP	$Z_{I_1} = -j\sqrt{Z_{oe}Z_{oo}}\cot\theta$	$\cosh\alpha = \dfrac{Z_{oe}+Z_{oo}}{Z_{oe}-Z_{oo}}$

Fig. 2(c).—Image parameters for coupled transmission line filters.

When these equations are solved for the mode currents in terms of the terminal currents, it is found that

$$\begin{aligned} i_1 &= \tfrac{1}{2}(I_1 + I_2) \\ i_2 &= \tfrac{1}{2}(I_1 - I_2) \\ i_3 &= \tfrac{1}{2}(I_4 + I_3) \\ i_4 &= \tfrac{1}{2}(I_4 - I_3). \end{aligned} \tag{6}$$

Since constant-current generators having infinite internal impedance are used in this derivation, each terminal voltage is the sum of all the mode voltages at that terminal. Thus

$$\begin{aligned} V_1 &= (v_{a_1} + v_{a_2} + v_{a_3} + v_{a_4})\big|_{z=o} \\ V_2 &= (v_{b_1} + v_{b_2} + v_{b_3} + v_{b_4})\big|_{z=o} \\ V_3 &= (v_{b_1} + v_{b_2} + v_{b_3} + v_{b_4})\big|_{z=l} \\ V_4 &= (v_{a_1} + v_{a_2} + v_{a_3} + v_{a_4})\big|_{z=l}. \end{aligned} \tag{7}$$

When (1)–(4) and (6) are substituted in (7), the coefficients of I_1, I_2, I_3, and I_4 are easily identified as the elements of the impedance matrix. Performing this operation, it is found that the matrix elements are

$$\begin{aligned} Z_{11} = Z_{22} = Z_{33} = Z_{44} &= -j(Z_{oe} + Z_{oo})\frac{\cot\theta}{2} \\ Z_{12} = Z_{21} = Z_{34} = Z_{43} &= -j(Z_{oe} - Z_{oo})\frac{\cot\theta}{2} \\ Z_{13} = Z_{31} = Z_{24} = Z_{42} &= -j(Z_{oe} - Z_{oo})\frac{\csc\theta}{2} \\ Z_{14} = Z_{41} = Z_{23} = Z_{32} &= -j(Z_{oe} + Z_{oo})\frac{\csc\theta}{2} \end{aligned} \tag{8}$$

where θ is the electrical length of the coupled wires.

The admittance matrix may also be derived by substituting a double-T configuration of voltage generators at each end for the double-π configuration of constant current generators used above. The results of this analysis show that the elements of the admittance matrix are

$$\begin{aligned} Y_{11} = Y_{22} = Y_{33} = Y_{44} &= -j(Y_{oo} + Y_{oe})\frac{\cot\theta}{2} \\ Y_{12} = Y_{21} = Y_{34} = Y_{43} &= -j(Y_{oo} - Y_{oe})\frac{\cot\theta}{2} \\ Y_{13} = Y_{31} = Y_{24} = Y_{42} &= -j(Y_{oo} - Y_{oe})\frac{\csc\theta}{2} \\ Y_{14} = Y_{41} = Y_{23} = Y_{32} &= -j(Y_{oo} + Y_{oe})\frac{\csc\theta}{2}. \end{aligned} \tag{9}$$

Coupled Transmission-Line Filters

There are ten filters that can be obtained from a pair of coupled strip lines by placing open or short circuits on various terminal pairs, or by connecting ends of the lines together. Fig 2(a), (b), and (c), on this page and the previous page, show single sections of the ten possible coupled transmission-line filters together with their image parameters. In the schematic diagrams of the coupled line filters, the input and output terminal pairs are designated by small open circles. The image impedance, or admittance, seen looking into each of

these terminal pairs is also shown near the terminal pair. Open-circuited terminal pairs of the coupled lines are shown with no connection in the filter schematic diagram, while short-circuited terminal pairs are designated with the standard grounding symbol.

Reference to Fig. 2 shows that it is possible to obtain low-pass, band-pass, and all-stop filters from a pair of coupled transmission lines. The low-pass filter 1 has an infinite number of pass bands centered about multiples of π, while the band-pass filters 2, 3, and 4 have an infinite number of pass bands centered about odd multiples of $\pi/2$. It is interesting to note that the bandwidth of the three band-pass filters is the same, while the bandwidth of the low-pass filter is just half that of the band-pass filters. Inspection of Fig. 2 also shows that there are close relationships among the image impedances of these filters. In particular, the product of the image impedances Z_{I_1} and Z_{I_2} of the unsymmetrical filters 1, 4, and 8 are each equal to $Z_{oo}Z_{oe}$. Furthermore, the product of the image impedances of the dual symmetrical filters 2 and 3, 5 and 6, and 9 and 10 are also equal to $Z_{oe}Z_{oo}$. Finally, the square of the image impedance of the symmetrical all-pass filter 7 is equal to $Z_{oe}Z_{oo}$.

Filter 8 does not have much practical utility; however, it does have interesting property of possessing an infinite image attenuation at all frequencies. Filters 9 and 10 are not very useful by themselves, but they can be made into band-pass filters by adding suitable reactive elements to their terminals. For example, the equivalent circuit of filter 9 is a symmetrical π composed of inductances. The susceptance of the inductances in each of the shunt arms is $-Y_{oe}\cot\theta$, while the susceptance of the series arm is

$$\frac{-(Y_{oo}-Y_{oe})\cot\theta}{2}.$$

The addition of series capacitances converts filter 9 into a well-known type of band-pass filter. The equivalent circuit of filter 10 is a symmetrical T network of capacitances. Each of the series capacitances has a reactance of $-Z_{oo}\cot\theta$, while the shunt capacitance has a reactance of

$$\frac{-(Z_{oe}-Z_{oo})\cot\theta}{2}.$$

In this case, series inductances must be added to this filter to convert it into a band-pass filter.

The image-parameter design equations presented in Fig. 2 are obtained in the following manner. First, the four-element impedance or admittance matrix of the filters is obtained from the four network equations

$$[V] = [Z][I] \tag{10}$$

or

$$[I] = [Y][V] \tag{11}$$

by applying the appropriate boundary conditions. Here $[V]$ and $[I]$ are four-element column matrices, while $[Z]$ and $[Y]$ are sixteen-element square matrices. For example, in filter 7 if it is assumed that terminal 3 and 4 are connected, the boundary conditions are $V_3 = V_4$ and $I_3 = -I_4$. In all the other filters the boundary conditions are $V=0$ or $I=0$ at terminals that are short-circuited or open-circuited, respectively. Second, the image impedance, Z_I, or image admittance, Y_I, and image transfer constant $(\alpha+j\beta)$ are calculated from the elements of the resulting four-element impedance matrix Z' or admittance matrix Y' by the following relations

$$Z_{I_1} = \left(Z_{11}'^2 - \frac{Z_{11}'Z_{12}'^2}{Z_{22}'}\right)^{1/2}, \quad Z_{I_2} = \left(Z_{22}'^2 - \frac{Z_{22}'Z_{12}'^2}{Z_{11}'}\right)^{1/2},$$

$$\cosh(\alpha + j\beta) = \frac{(Z_{11}'Z_{22}')^{1/2}}{Z_{12}'} \tag{12}$$

or

$$Y_{I_1} = \left(Y_{11}'^2 - \frac{Y_{11}'Y_{12}'^2}{Y_{22}'}\right)^{1/2}, \quad Y_{I_2} = \left(Y_{22}'^2 - \frac{Y_{22}'Y_{12}'^2}{Y_{11}'}\right)^{1/2},$$

$$\cosh(\alpha + j\beta) = \frac{Y(_{11}'Y_{22}')^{1/2}}{Y_{12}'}. \tag{13}$$

Physical Layout of Coupled-Strip-Line Filters

In most applications it is necessary to cascade several of the basic filter sections shown in Fig. 2 in order to achieve the desired performance from the filter. Fig. 3 illustrates the way these basic filter sections might be cascaded using strip line techniques. It is seen that where the input and output of basic sections occur at opposite ends of the strips (*i.e.*, as in filters 1, 2, 3, 5, 6, and 8) any number of sections may be cascaded. However, when the input and output of a single section occur at the same end, (*i.e.*, as in filters 4, 7, and 10) only two sections may be cascaded.

The image impedance of the coupled strip line filters is either higher or lower than the characteristic impedance of an isolated strip. Therefore, it is necessary to connect the filters to strips having different widths than the coupled strips, in order to reduce the mismatch loss at the terminals. For example, when the image impedance of the filter is less than the characteristic impedance of an isolated strip, the connecting strip is made wider than the coupled strips and, when the image impedance of the filter is greater than the characteristic impedance of an isolated strip, the connecting line is made narrower. The proper width of the connecting lines is illustrated for the filters in Fig. 3. At the bottom of Fig. 3 is shown the way in which the all-stop filters 9 and 10 may be converted to band-pass filters by adding series capacitors and series inductors, respectively.

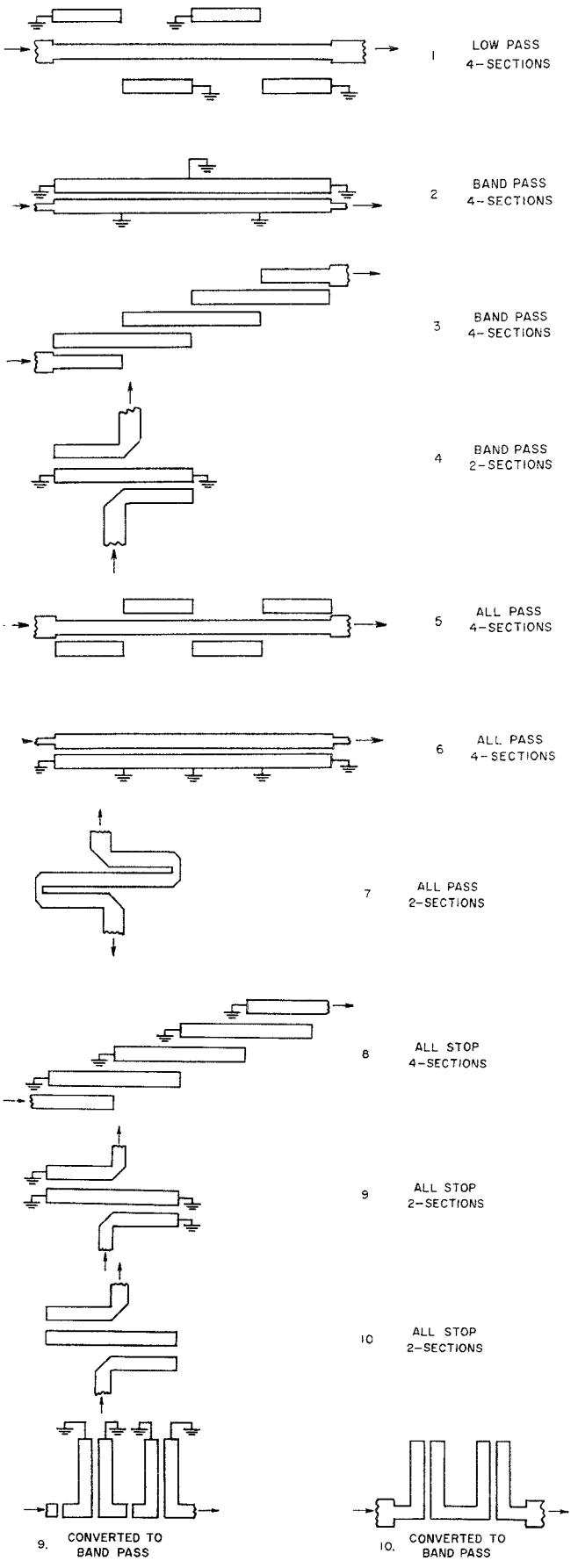

Fig. 3.—Physical layout of coupled strip line filters.

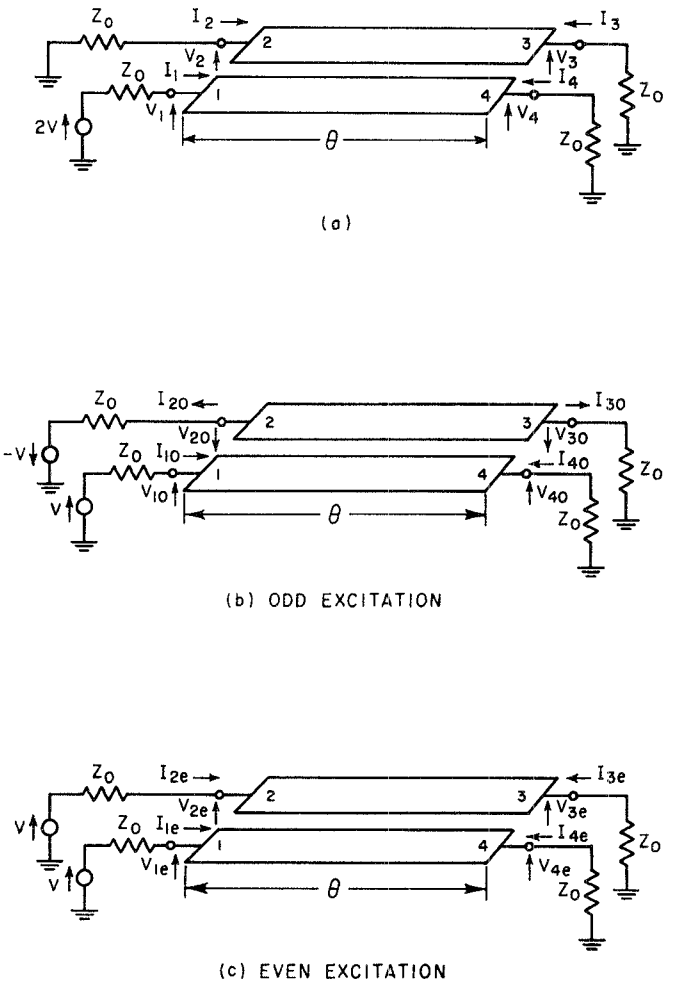

Fig. 4.—Strip line directional coupler with even and odd excitation.

Coupled-Strip-Line Directional Couplers

When the four terminal pairs of the coupled strip transmission lines illustrated in Fig. 1 are terminated in the proper constant resistance, the device behaves as a directional coupler with constant input impedance and infinite directivity at all frequencies, and for all degrees of coupling.[6] In this coupler energy is coupled backward instead of forward. Hence, if a signal is fed into one terminal pair, the coupled signal emerges from the adjacent terminal pair and no signal emerges from the diagonally opposite terminal pair.

The characteristics of this directional coupler can be determined rigorously from the impedance matrix. However, its behavior will be derived here from certain symmetry arguments, because it is believed that such a presentation gives the best physical picture of the directional coupler operation.

A simplified schematic diagram of the directional coupler is shown at the top of Fig. 4 with resistance terminations Z_o at each terminal. The coupler is ex-

[6] Oliver and Knechtli, *loc. cit.*, have also recently analyzed coupled transmission-line directional couplers and shown that they can be designed to have infinite directivity and constant input impedance for all degrees of coupling.

cited with a voltage $2V$ in series with terminal 1. At the bottom of Fig. 2, the same directional coupler is shown in two different states of excitation. In the odd excitation, out-of-phase voltages are applied in series with terminals 1 and 2, while the even excitation applies in-phase voltages in series with these terminals. Through the principle of superposition it may be seen that the behavior of the directional coupler with voltage $2V$ applied in series with terminal 1 can be obtained from its behavior with even and odd voltage excitations.

It is seen that the characteristic impedance of one of these strips to ground in the odd excitation is Z_{oo}, while the characteristic impedance of a strip to ground in the even excitation is Z_{oe}. In order for the directional coupler to have a perfect match at all frequencies it is necessary that the input impedance Z_{in} be equal to Z_o. Applying the principal of superposition, it is seen that the input impedance of the directional coupler terminated in Z_o can be written as

$$Z_{\text{in}} = \frac{V_{1o} + V_{1e}}{I_{1o} + I_{1e}} = \frac{\dfrac{Z_{1o}}{Z_o + Z_{1o}} + \dfrac{Z_{1e}}{Z_o + Z_{1e}}}{\dfrac{1}{Z_o + Z_{1o}} + \dfrac{1}{Z_o + Z_{1e}}}, \tag{14}$$

where

$$Z_{1o} = Z_{oo}\frac{(Z_o + jZ_{oo}\tan\theta)}{Z_{oo} + jZ_o\tan\theta} \tag{15}$$

and

$$Z_{1e} = Z_{oe}\frac{(Z_o + jZ_{oe}\tan\theta)}{Z_{oe} + jZ_o\tan\theta}. \tag{16}$$

When (15) and (16) are substituted in (14), it is found that $Z_{1n} = Z_o$ when

$$Z_o = (Z_{oo}Z_{oe})^{1/2}. \tag{17}$$

This characteristic impedance of the coupler, $(Z_{oe}Z_{oo})^{1/2}$, is always less than the characteristic impedance of a single strip line of the same width. Therefore, the width of the lines connecting to the coupler is required to be slightly wider than the coupled strips. Although for couplings weaker than -15 db, the change in width is negligible.

Under the condition that $Z_o = (Z_{oe}Z_{oo})^{1/2}$, the voltage appearing at terminal 1 of the coupler is $V_1 = V$. The voltages $V_{2e} = V_{1e}$ and $V_{3e} = V_{4e}$ may be determined from the straightforward analysis of a transmission line of length θ, and characteristic impedance Z_{oe} terminated at either end by an impedance $(Z_{oe}Z_{oo})^{1/2}$ and fed by a voltage V. Likewise the voltages $V_{2o} = -V_{1o}$ and $V_{3o} = -V_{4o}$ may be determined from a similar analysis of a transmission line of length θ and characteristic impedance Z_{oo} terminated by $(Z_{oe}Z_{oo})^{1/2}$. The results of this analysis show that

$$V_2 = V_{2e} - V_{2o} = j\frac{V\sin\theta\left[\sqrt{\dfrac{Z_{oe}}{Z_{oo}}} - \sqrt{\dfrac{Z_{oo}}{Z_{oe}}}\right]}{2\cos\theta + j\sin\theta\left[\sqrt{\dfrac{Z_{oe}}{Z_{oo}}} + \sqrt{\dfrac{Z_{oo}}{Z_{oe}}}\right]}, \tag{18}$$

$$V_3 = V_{3e} - V_{3o} = 0 \tag{19}$$

$$V_4 = V_{4e} - V_{4o} = \frac{2V}{2\cos\theta + j\sin\theta\left[\sqrt{\dfrac{Z_{oe}}{Z_{oo}}} - \sqrt{\dfrac{Z_{oo}}{Z_{oe}}}\right]}. \tag{20}$$

The maximum coupled voltage, V_2, occurs when the coupler is a quarter wavelength long (*i.e.*, $\theta = 90°$). Therefore, from (18) a maximum coupling coefficient k may be defined as

$$\left|\frac{V_2}{V}\right| = k = \frac{\dfrac{Z_{oe}}{Z_{oo}} - 1}{\dfrac{Z_{oe}}{Z_{oo}} + 1}. \tag{21}$$

With this substitution, the voltage at terminal 2 can be written as

$$V_2 = V\frac{jk\sin\theta}{\sqrt{1 - k^2}\cos\theta + j\sin\theta} \tag{22}$$

while the voltage at terminal 4 becomes

$$V_4 = \frac{V\sqrt{1 - k^2}}{\sqrt{1 - k^2}\cos\theta + j\sin\theta}. \tag{23}$$

Eqs. (22) and (23) are the same as those obtained by Oliver.[4] Reference to his Fig. 6 or to (22) above shows that for small values of k the coupler will operate over a 3 to 1 frequency band between 3 db points, while for stronger couplings even wider bandwidths of operation are obtained.

Coupled Transmission Line Impedances Z_{oe} and Z_{oo}

The characteristic impedances Z_{oe} and Z_{oo} of infinitesimally thin coupled strip lines have been calculated rigorously by Cohn[7] who presents the information in the form of a nomogram. The reader is also referred to Cohn's paper for approximate values of Z_{oe} and Z_{oo} for thick strips and strips printed on dielectric sheets.

In applications where these components must be operated at high rf potentials, the possibility of breakdown is minimized by using round conductors instead of strips. Approximate formulas for Z_{oe} and Z_{oo} for the round conductors have been derived by Honey.[8]

[7] S. B. Cohn, "Shielded coupled-strip line," Trans. IRE, vol. MTT-3, pp. 29–38; October, 1955.

[8] R. C. Honey, Stanford Research Institute, private communications.

He finds that

$$Z_{oe} - Z_{oo} = \frac{120}{\sqrt{\epsilon_r}} ln \coth \frac{\pi s}{2b} \quad (24)$$

$$Z_{oe} + Z_{oo} = \frac{120}{\sqrt{\epsilon_r}} ln \coth \frac{\pi d}{4b} \quad (25)$$

where s = center to center spacing of the wires, d = wire diameter, b = ground plane spacing, and ϵ_r = relative dielectric constant of medium surrounding the wires. For configurations of coupled lines that are not amenable to analysis it is always possible to determine Z_{oo} and Z_{oe} from measurements of the static capacity of the strips. Thus

$$Z_{oo} = \frac{100\sqrt{\epsilon_r}}{3C_{oo}} = \frac{100\sqrt{\epsilon_r}}{3[C_{22} - C_{23}]} \quad (26)$$

while

$$Z_{oe} = \frac{100\sqrt{\epsilon_r}}{3C_{oe}} = \frac{100\sqrt{\epsilon_r}}{3[C_{22} + C_{23}]} \quad (27)$$

where

C_{oo} = one half the capacity between the two center conductors ($\mu\mu$f/cm),

C_{oe} = one half the capacity between the parallel combination of the two center conductors and ground ($\mu\mu$f/cm),

C_{22} = coefficient self capacity ($\mu\mu$f/cm) of either of the center conductors,

C_{23} = coefficient of induction ($\mu\mu$f/cm) between the two center conductors (a negative quantity).

The capacity C_{22} is easily measured as the capacity between either strip and ground when the other strip is grounded, while the capacity $C_{22} \mp C_{23}$ is just one half the capacity between the parallel combination of the two center conductors and ground.

ACKNOWLEDGEMENT

The work reported in this paper was conducted under Contract No. AF 33(038)-7850 sponsored by the Air Force Cambridge Research Center, and Contract No. DA 36-039-sc-63232 and DA 36-039-sc-64625 sponsored by the Signal Corps Engineering Laboratories.

Absolute Measurement of Receiver Noise Figures at UHF*

E. MAXWELL† AND B. J. LEON†

Summary—**Absolute measurements of noise-figures in the UHF range are described, using hot and cold thermal sources as standards. It was found that the noise temperature of the T-5 6 watt fluorescent tube is 16.1 ±0.6 db above $kT\Delta\nu$. Noise diodes were found to be in error at these frequencies by approximately 1 db.**

INTRODUCTION

THE noise figure of a receiver is conventionally defined as

$$F = \frac{\text{Noise power output of receiver}}{\text{Receiver gain} \times \text{available noise power from source}}.$$

It is measured either by comparing the noise power produced by the receiver with a signal from a calibrated signal generator, or with an external source of noise power of known intensity. The signal generator technique is straightforward but difficult to do precisely and requires that the "noise bandwidth" of the receiver be determined.[1] The second technique, which uses a calibrated noise generator, is simpler to apply and is usually capable of greater precision provided that a reliable standard of noise is available. Two types of noise generators which are primary standards, and hence self-calibrating, are the thermal source and the noise diode. The thermal source is simply a resistor at some temperature, T, which is capable of delivering noise power $kT\Delta\nu$ to some external device. Although simple in principle it is obviously restricted to laboratory use and has relatively low noise output. The diode noise source is a temperature limited diode. It can be shown[2] that the diode current contains a shot noise component whose means square value is

$$\bar{i}^2 = 2eI\Delta\nu$$

in the frequency interval $\Delta\nu$. e is the electronic charge and I the dc diode current. If the diode is shunted by a resistance R the combination is a noise generator with available power $2eIR\Delta\nu$. At frequencies high enough, so that the transit time of the electrons may not be neg-

* The research in this document was supported jointly by the Army, Navy, and Air Force under contract with the M.I.T. This paper was presented at the URSI-IRE symposium held in Washington, D. C.; May 2–5; 1956.

† Massachusetts Institute of Technology, Cambridge, Mass.

[1] G. E. Valley and H. Wallman, "Vacuum Tube Amplifiers," McGraw-Hill Book Co., New York, p. 695; 1948.

[2] *Ibid.*, p. 701.